

ARTICLES

An Electron Energy-Loss Spectrometry Study of Charge Compensation in $\text{LiNi}_{0.8}\text{Co}_{0.2}\text{O}_2$

J. Graetz,* C. C. Ahn, R. Yazami, and B. Fultz

Division of Engineering and Applied Science, California Institute of Technology, Pasadena, California 91125

Received: July 9, 2002; In Final Form: January 6, 2003

Changes in the electronic structure of $\text{Li}_{1-x}\text{Ni}_{0.8}\text{Co}_{0.2}\text{O}_2$ during delithiation (charge) are elucidated by changes in the O K-edge and transition-metal (TM) $\text{L}_{2,3}$ -edge. Electron energy-loss spectrometry was used to investigate the O 2p and TM 3d occupancy over a wide range of lithium concentrations. Quantitative analysis of the TM $\text{L}_{2,3}$ white lines indicates that the Ni ion accommodates no more than one-half of an electron, whereas the net Co valence is unaffected by delithiation. In contrast with the small changes observed in the TM $\text{L}_{2,3}$ -edge, a large decrease in state occupancy is observed in the near-edge structure of the O K-edge, suggesting that much of the electron charge is accommodated by the anion.

1. Introduction

Lithium transition-metal oxides, LiTMO_2 , are in widespread use as cathodes in secondary lithium batteries. These high-voltage cathodes maintain stable electrochemical behavior upon lithium deintercalation and exhibit excellent cycle life. $\text{LiNi}_{1-y}\text{Co}_y\text{O}_2$ ($0 < y < 1$) has a layered structure with rhombohedral symmetry and belongs to the $R\bar{3}m$ space group. The compound $\text{LiNi}_{0.8}\text{Co}_{0.2}\text{O}_2$ is a promising cathode for lithium batteries. It has the same layered structure as LiCoO_2 but with a substitution of Ni atoms at the Co sites. In $\text{LiNi}_{0.8}\text{Co}_{0.2}\text{O}_2$, the Ni and Co ions are both octahedrally coordinated by O ions and occupy the same crystallographic sites. This material is an improvement over LiNiO_2 , because it combines a high cycling capacity with safe operating conditions even in the delithiated charge state. $\text{LiNi}_{0.8}\text{Co}_{0.2}\text{O}_2$ remains as a single phase during deep lithium deintercalation, allowing reversible cycling from $\text{Li}_{1.0}$ to $\text{Li}_{0.4}$.¹ Also, $\text{LiNi}_{0.8}\text{Co}_{0.2}\text{O}_2$ is less susceptible to cationic disorder (TM ions occupying Li sites) than the LiNiO_2 system. $\text{LiNi}_{0.8}\text{Co}_{0.2}\text{O}_2$ has a slightly lower voltage versus lithium, when compared to LiCoO_2 ; consequently, electrochemical cells are less prone to electrolyte decomposition. Finally, the reduction of Co also allows for a cheaper, more environmentally friendly cathode.

During electrochemical discharge, Li ions and their associated electrons are intercalated into the TMO_2 host. There have recently been several investigations into how the intercalated lithium affects the electronic structure of the host.^{1–15} The results of these studies have led to recent debate over the amount of charge transferred to the O and TM ions. Analyses of the TM core edges, using X-ray absorption spectroscopy (XAS), magnetic susceptibility, electronic conductivity, and thermoelectric measurements, have shown that, upon lithium deintercalation, the TM ion is oxidized to the tetravalent state.^{1–3,9,10} Studies of the $\text{LiNi}_{1-y}\text{Co}_y\text{O}_2$ system suggest that, during discharge, the Ni ions are immediately oxidized to the tetravalent state, whereas

the Co oxidation occurs only in the heavily delithiated state.^{1–3} In $\text{LiNi}_{0.8}\text{Co}_{0.2}\text{O}_2$, the preferential oxidation of Ni over Co is attributed to the position of the Fermi level, which lies within the energy gap between the $\text{Ni}^{2+}/\text{Ni}^{3+}$ and $\text{Ni}^{3+}/\text{Ni}^{4+}$ redox couples. It is argued that the Fermi level drops into the $\text{Ni}^{3+}/\text{Ni}^{4+}$ band during the early stages of delithiation and the nickel is oxidized. The t_{2g} band of Co appears at a lower energy, requiring the removal of up to 80% of the Li atoms before the Fermi level is lowered sufficiently for Co oxidation.¹ Although there is general agreement that the Co ion participates little in the redox processes that occur during cycling, the behavior of the Ni ion is still not well understood. The notion of a trivalent Ni ion in the fully lithiated material has been disputed by recent results of Montoro et al., which suggest that, in $\text{LiNi}_{0.5}\text{Co}_{0.5}\text{O}_2$, the Ni ions are divalent and are partially oxidized to a trivalent state during delithiation.¹¹

Absorption studies using hard X-rays have been used to investigate the electronic structure around the TM ions. However, these studies are unable to measure electronic transitions with low absorption energies, such as those contributing to the O K-edge. Therefore, these measurements are relatively insensitive to the atomic states of O. More indirect experiments, such as magnetic measurements, can be difficult to interpret and may be misleading because changes in the spin density, or the number of unpaired electrons around an ion, are not necessarily correlated with changes in the charge density.

Soft X-ray absorption and transmission electron energy-loss spectroscopy (EELS) are well suited for studying the electronic structure around the O and TM ions at different states of lithiation. Recent studies of the O K-edge and Ni,Co $\text{L}_{2,3}$ -edges have shown that the O ion is responsible for accommodating much of the Li 2s electron during intercalation.^{12–15} These studies suggest an almost-constant net charge density about the TM ion, with significant changes in occupancy of the O 2p band. The details of the redox energies of the individual TM ions appear to be subordinate to changes occurring in the O valence.

First-principles calculations by Wolverton and Zunger have shown that, in LiCoO_2 , the total charge density around the Co

* To whom correspondence should be addressed. E-mail address: graetz@caltech.edu.

ion is unaffected by the lithium concentration. This behavior is attributed to a rehybridization of the Co–O bond, which produces invariant energy levels and electronic stability over a wide range of lithium concentration.¹⁶ Other first-principles calculations of LiCoO_2 have suggested that much of the Li 2s electron is donated to the O, allowing the Co valence to remain predominately in the trivalent state.^{17–19} These ab initio studies add insight into the experimental results for the ordered LiCoO_2 and LiNiO_2 systems. However, calculations on a disordered distribution of Ni and Co atoms are not practical, because of the complexity of the unit cell of $\text{Li}(\text{Ni},\text{Co})\text{O}_2$. Here, we report results from an experimental investigation using transmission EELS to elucidate changes in the electronic structure of $\text{Li}_{1-x}\text{Ni}_{0.8}\text{Co}_{0.2}\text{O}_2$ with the amount of lithium removed, x .

2. Experimental Section

Samples were prepared by chemically charging (delithiating) $\text{LiNi}_{0.8}\text{Co}_{0.2}\text{O}_2$ powders, which were provided by Enax Inc. A previous investigation of the core edges of $\text{Li}_{1-x}\text{CoO}_2$ revealed similar results for chemically and electrochemically delithiated samples. However, chemically prepared samples are preferred, because spectral artifacts from binders and conductive diluents can be eliminated. In this study, an aqueous solution of potassium persulfate ($\text{K}_2\text{S}_2\text{O}_8$) was used as an oxidant. The lithium concentration was altered by mixing powders of $\text{LiNi}_{0.8}\text{Co}_{0.2}\text{O}_2$ into different amounts of the oxidizing solution, and samples were agitated for ~ 24 h at 60°C . The delithiated powders were filtered and rinsed several times in water to remove all the $\text{K}_2\text{S}_2\text{O}_8$. To remove the residual water, the samples were dried in air at 60°C for 24 h and stored in an argon atmosphere. The elemental analysis of the bulk material was performed using inductively coupled plasma–mass spectrometry (ICP-MS). Two methods were employed to determine the final lithium concentrations in $\text{Li}_{1-x}\text{Ni}_{0.8}\text{Co}_{0.2}\text{O}_2$. First, the amount of lithium removed from the stoichiometric material, x , was measured in the $\text{K}_2\text{S}_2\text{O}_8$ solution using ICP-MS. Second, the amount of lithium remaining in the delithiated oxides ($1 - x$) was measured by ICP-MS. A structural analysis was performed using X-ray diffraction (XRD). Powder XRD patterns were acquired with an Inel model CPS-120 diffractometer, using Co K α radiation ($\lambda = 1.790$ Å). The XRD results of the delithiated samples exhibited an (003) line width of $\Delta 2\theta = 0.3^\circ$. These results were compared with those of Ronci et al., to ensure that the structure was not altered during delithiation and to confirm the ICP-MS measurements.²⁰

Transmission electron microscopy and EELS measurements require an electron-transparent sample. To ensure that some of the particles in the $\text{Li}_{1-x}\text{Ni}_{0.8}\text{Co}_{0.2}\text{O}_2$ were suitably thin, the powders were crushed with a mortar and pestle in Fluorinert and the fine particles were dispersed onto a holey carbon grid. The EELS spectra were acquired using a Gatan model 666 parallel-detection spectrometer in a Philips model EM 420 transmission electron microscope operated at 100 keV. The spectra were acquired with diffraction coupling (image mode), at a dispersion of 0.5 eV per channel. A large collection angle of ~ 100 mrad was used to ensure spectral contributions from the entire Bethe ridge. The energy resolution was ~ 1.5 eV.

3. Results

The various core edges for the five $\text{Li}_{1-x}\text{Ni}_{0.8}\text{Co}_{0.2}\text{O}_2$ samples are shown in Figures 1–3. Detector artifacts were removed by dividing out the instrument response. The full energy-loss spectra ($0 \leq E \leq 950$ eV) were then deconvolved using the Fourier-log method.²¹ (The deconvolution process removes the

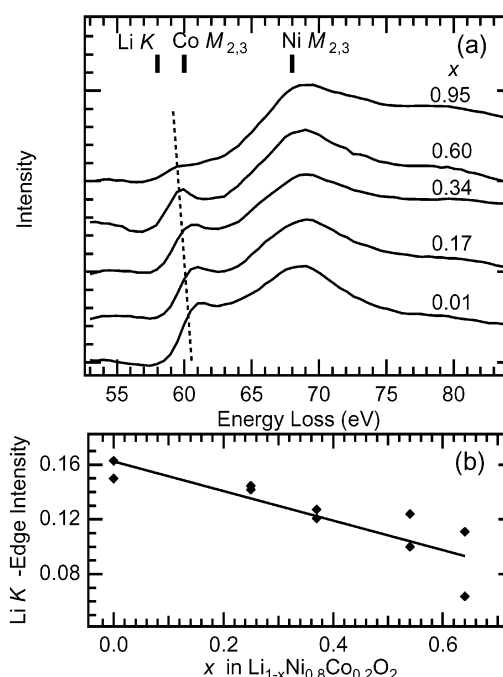


Figure 1. (a) Li K-edge from $\text{Li}_{1-x}\text{Ni}_{0.8}\text{Co}_{0.2}\text{O}_2$, labeled by x . The dashed line connects the Li K-edge peaks. (b) Normalized Li K-edge intensity vs measured lithium concentration (ICP-MS).

effects from plural scattering that distort the shape of the near-edge structure.) Finally, a background was fit to the pre-edge region, using a power-law decay function, and subtracted from beneath the core edges.

The lowest-lying core edges for the $\text{Li}_{1-x}\text{Ni}_{0.8}\text{Co}_{0.2}\text{O}_2$ system are shown in Figure 1a. The Li K-edge onset occurs at ~ 58 eV, which is shifted by ~ 3 eV with respect to lithium metal. The shift to higher energies in lithium-metal oxides is the result of the ionic bonding between the lithium and the host structure. The loss of the Li 2s electron reduces the screening of the nuclear charge, thereby increasing the binding energy of the core electron and increasing the ionization energy. This region of the energy-loss spectrum also contains contributions from the Co and Ni $\text{M}_{2,3}$ -edges at ~ 60 and ~ 68 eV, respectively. The Co and Ni $\text{M}_{2,3}$ -edges appear to be unaffected by the lithium concentration. The Ni and Li edges are adequately separated in energy, and although the Co and Li edges overlap, the contribution from Co is small enough so that changes at the Li K-edge can be resolved clearly. As expected, this figure shows a decrease in the intensity of the Li K-edge as lithium is extracted from the material.

ICP-MS and XRD results from the bulk powders have provided averaged information on the chemical composition of the delithiated samples. However, energy-loss spectra are acquired from areas of the sample $< 1 \mu\text{m}^2$ in size, so the composition of the analyzed region may be different from the bulk. The spectra of Figure 1a were used to calibrate the Li K-edge intensity with the lithium concentration. The integrated intensity of the Li K-edge was measured using a 5 eV window and normalized to the invariant Ni $\text{M}_{2,3}$ -edge. Figure 1b shows the linear relationship found between the Li K-edge intensity and the bulk lithium concentration, as measured by ICP-MS. Using this calibration, the quantified Li K-edge intensity of a delithiated particle was then used to determine the lithium concentration of the region under analysis, thus avoiding errors due to compositional heterogeneities in the powders. Figure 1b shows a consistent edge intensity in the fully lithiated powders ($\pm 4\%$). The largest variations in the edge intensities, $\pm 30\%$,

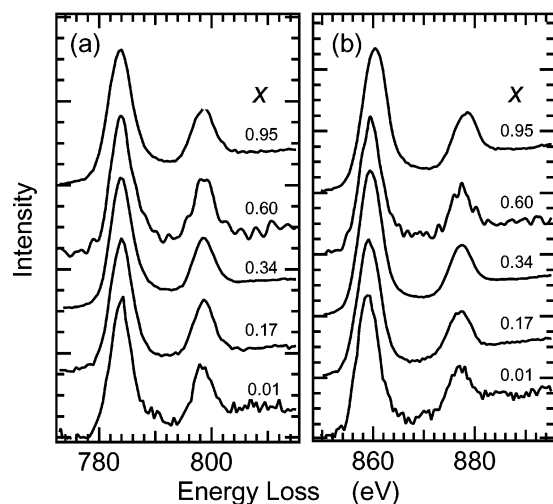


Figure 2. (a) Co and (b) Ni $L_{2,3}$ white lines from $\text{Li}_{1-x}\text{Ni}_{0.8}\text{Co}_{0.2}\text{O}_2$, labeled by x .

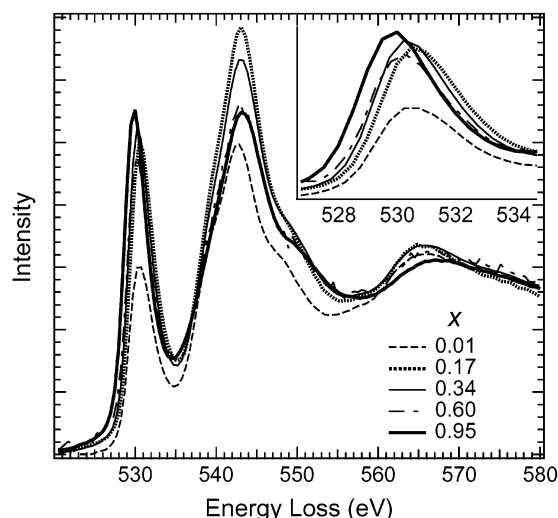


Figure 3. O K-edge from $\text{Li}_{1-x}\text{Ni}_{0.8}\text{Co}_{0.2}\text{O}_2$, labeled by x . Inset shows expanded view of the prepeak.

were found in the most delithiated sample. A linear fit to these data does not extrapolate to zero at $x = 1.0$, because of some interference from the Co $M_{2,3}$ -edge.

The Co and Ni $L_{2,3}$ -edges for the delithiated samples are shown in panels a and b, respectively, in Figure 2. The edge onset is characterized by two sharp peaks, which are the result of transitions from the $2p_{1/2}$ and $2p_{3/2}$ energy levels into unoccupied 3d states. In measuring the integrated white lines, the free-electron-like contributions to the core edges were approximated as step functions and subtracted from the total intensity. The Co and Ni white lines were normalized to integration windows of 40 and 50 eV, respectively, just above the L_2 -edge. To maximize the energy resolution over the fixed detector array, the spectra were acquired in two intervals and matched in energy scale after the acquisition. The Co $L_{2,3}$ white lines were used for energy calibration, so the TM and O edge onset energies are not reliable.

The O K-edge for five $\text{Li}_{1-x}\text{Ni}_{0.8}\text{Co}_{0.2}\text{O}_2$ samples is shown in Figure 3. The edge onset is characterized by a large prepeak at 530 eV, corresponding to a σ^* transition. The unoccupied σ antibonding state is the consequence of a hybridization of the O 2p band with the highly localized TM 3d states. A proposed energy diagram of the TM 3d–O 2p bonding is shown in Figure 4. In Figure 3, the structure of the main peak at 538 eV is due

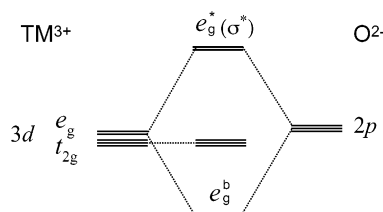


Figure 4. Molecular orbital diagram of the TM–O bonding in LiTMO_2 .

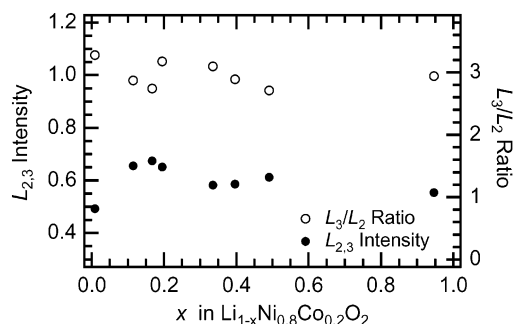


Figure 5. Co $L_{2,3}$ white-line intensity and L_3/L_2 ratio.

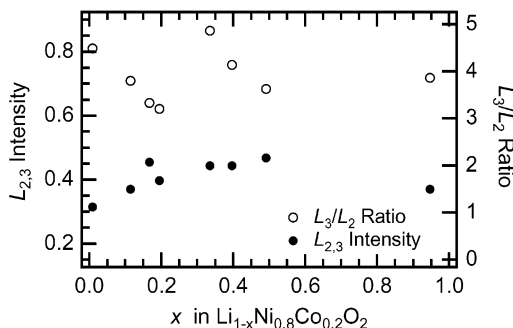


Figure 6. Ni $L_{2,3}$ white-line intensity and L_3/L_2 ratio.

to intrashell multiple scattering of the first O shell.^{22–24} The spectral intensities were normalized to a 10 eV window 40 eV above the edge onset, and the deintercalation value, x , was measured using the intensity of the Li K-edge.

4. Discussion

The Co and Ni $L_{2,3}$ white lines shown in panels a and b, respectively, in Figure 2 are essentially unchanged with changes in lithium concentration. The spectral intensity of the white lines is governed by $2p \rightarrow 3d$ transitions. The integrated white-line intensity is a measure of the holes in the localized 3d states around the transition metal. The Co and Ni white-line intensities are shown in Figures 5 and 6, respectively. These plots show an almost-constant white-line intensity over a wide range of lithium concentration. A linear fit to the Co $L_{2,3}$ intensity is essentially constant over the delithiated series, whereas the Ni white-line intensity increased by $\sim 5\%$. The invariant Co white-line intensity indicates a constant 3d band occupancy during delithiation. The increase in the Ni white-line intensity implies a depletion of the 3d band, which suggests that the Ni ions may compensate for some of the Li charge. The calibration of the relationship of white-line intensity and 3d occupancy in transition-metal oxides was originally performed by Stolojan et al.²⁵ An inverse linear relationship between the integrated white-line intensity and the atomic number (d occupancy) is well documented for the 3d transition metals.^{26,27} The Ni $L_{2,3}$ intensities of the delithiated samples were compared with our own analysis of the transition-metal oxide standards, based on

the original study.²⁵ The Ni ions in the fully lithiated material were found to be predominately divalent. The 5% increase in the Ni white-line intensity corresponds to a change in the Ni valence of 0.20 electron over the delithiated series. This increase is based on the assumption that the oxidation of Ni occurs linearly from $0 \leq x \leq 1$. However, Montoro et al. have suggested that the oxidation of nickel reaches a plateau at $x \approx 0.5$, which is in agreement with the measured white-line intensities shown in Figure 6. Assuming such a saturation, a linear fit from $0 \leq x \leq 0.5$ suggests that the Ni ions may compensate up to 0.50 electron during lithiation.

The total intensity difference over the delithiated series (5% in Ni) is near the detectable limit, given the variations between points of similar lithium concentration. Therefore, the total charge compensation measured is not absolute but, instead, should be regarded as an upper bound. These charge compensation measurements apply to changes only occurring in the 3d band, because the transition probabilities are governed approximately by the dipole selection rule (Δl values less than or equal to ± 1). Intraband transitions are negligible, so the TM $L_{2,3}$ -edge is insensitive to the occupancy of the TM 4p states.

The ratio of the L_3 to L_2 lines yields information governing the interaction between the 2p core-hole and the 3d electrons. The p states have a degeneracy of $2j + 1$ and, therefore, the ratio of L_3 ($j = 3/2$) to L_2 ($j = 1/2$) has a theoretical value of 2. However, deviations from this value have been reported in 3d transition metals and their associated oxides. The nonstatistical value of the white-line ratio varies with oxidation state in the 3d transition metals.^{28,29} The Co and Ni L_3/L_2 ratios are shown in Figures 5 and 6, respectively. Although the absence of a perceptible trend in the Ni white-line ratios makes them difficult to interpret, the constant Co white-line ratios lends credence to the notion of an invariant Co valence, relative to delithiation.

The stability of the white lines suggests that the TM ions are not responsible for accepting all the Li charge and, therefore, implies that the O ions may play a significant role in charge compensation. In these LiTMO_2 compounds, the O 2p band is hybridized with the localized TM 3d band. Transitions to the O 2p holes are observed in the near-edge structure (530 eV) of the EELS spectra shown in Figure 3. This prepeak corresponds to transitions to a predominantly unoccupied σ^* molecular orbital. The availability of this transition requires a strong O 2p–TM 3d hybridization; therefore, the intensity of this peak is a measure of the covalency of the TM–O bond.^{30–32}

The O K-edges for the delithiated series (Figure 3) show an increase in the integrated intensity of the prepeak at 530 eV. These changes indicate an increase in unoccupied 2p states or, equivalently, a decrease in charge density around the O ions with delithiation. The behavior of the O K-edge corroborates the trends in the TM white lines and verifies the claim that the O ion compensates for much of the Li 2s electron. This method of charge compensation suggests the oxidation of oxygen, which is contrary to conventional chemistry. A resolution to this paradox, originally proposed by Wolverton and Zunger for LiCoO_2 , is that the delithiation drives the $\text{Co}^{3+} \rightarrow \text{Co}^{4+}$ redox process but simultaneous changes in the Co–O hybridization lead to a decrease in the charge density around the O ions.¹⁶ These calculations showed a constant charge density around the Co ion as the lithium content was reduced.¹⁶

The relationship between the number of O 2p holes and the state of charge is quantified in Figure 7, which compares the integrated intensity of the near-edge structure in $\text{LiNi}_{0.8}\text{Co}_{0.2}\text{O}_2$ with the lithium concentration. A linear fit was made to the

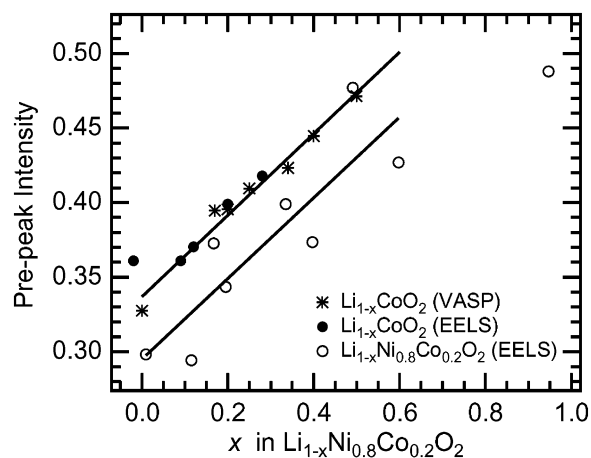


Figure 7. Normalized intensity of antibonding peak in the calculated O partial density of states (VASP) for $\text{Li}_{1-x}\text{CoO}_2$ and measured prepeak of the O K-edge (EELS) for $\text{Li}_{1-x}\text{CoO}_2$ and $\text{Li}_{1-x}\text{Ni}_{0.8}\text{Co}_{0.2}\text{O}_2$.¹⁴ The ionization cross sections were divided out of the experimental data.

data between $0 \leq x \leq 0.6$, to compare with previous results for LiCoO_2 . This fit reveals a 60% increase in the intensity of the O K near-edge structure. Previous EELS data for LiCoO_2 and the partial density of states (pdos), as calculated for LiCoO_2 using the VASP code, are also shown in Figure 7.¹⁴ The energy-loss data used in this plot were corrected for their inelastic form factor, which were calculated with Hartree–Slater wave functions. The simulated data were generated from the pdos of $\text{Li}_{1-x}\text{CoO}_2$ and were taken to be the integrated intensity of the lowest-lying peak above the Fermi energy. The plot shows that the intensity of the unoccupied antibonding state is correlated linearly to the lithium concentration. The slopes for the Co and (Ni,Co) systems are ~ 0.26 and ~ 0.28 , respectively. The difference in the initial intensity is likely due to the different number of O 2p holes present in the stoichiometric material of the two systems. The $\text{Li}(\text{Ni,Co})\text{O}_2$ material has fewer O 2p holes than does LiCoO_2 .

Van der Ven et al. recently showed that lithium intercalation into a CoO_2 host results in a polarization of the e_g^b bond between O and Co, with the bulk of the electron density residing around the O ion. It was also shown that the net charge about the O atom increases linearly as the lithium intercalation increases. Their relationship between the O valence and the lithium concentration exhibits a slope of 0.28–0.30,¹⁹ which is in agreement with our measured slopes for this system. This group has also shown that the net change about the Co ion is rather constant, relative to the lithium concentration.^{17–19} Their predicted behavior of the TM valence, relative to the lithium concentration, is in agreement with our measured white-line intensities.

5. Conclusion

The near-edge structure of the O K-edge exhibits large changes over a range of lithium content in $\text{Li}(\text{Ni,Co})\text{O}_2$. Smaller changes are observed in the Ni $L_{2,3}$ white lines, whereas no perceptible change was observed for the Co $L_{2,3}$ white lines. The Ni ions were found to be divalent in the fully lithiated state. The upper bound on the total charge transferred from the Li ions to the Ni ions was determined to be one-half of an electron, whereas no charge transfer to the Co ions was observed. These trends suggest that the O ion compensates for much of the depleted electronic charge during deintercalation of $\text{Li}(\text{Ni,Co})\text{O}_2$. This mechanism of charge compensation allows the net Co valence to remain constant and the Ni valence to change slowly

over a wide range of lithium concentration. The modest changes occurring in the electronic structure of the transition metals may be partially responsible for the structural stability of the transition-metal oxide (TMO_2) host during cycling.

Acknowledgment. We would like to thank Enax Inc. (Japan) for providing the $\text{LiNi}_{0.8}\text{Co}_{0.2}\text{O}_2$, and we are grateful to Reminex Inc. (Morocco) for the elemental analyses of the oxides. This work was supported by the Department of Energy, through Basic Energy Sciences Grant No. DE-FG03-00ER15035.

References and Notes

- (1) Saadoune, I.; Delmas, C. *J. Solid State Chem.* **1998**, *136*, 8.
- (2) Delmas, C.; Saadoune, I. *Solid State Ionics* **1992**, *370–375*, 53–56.
- (3) Balasubramanian, M.; Sun, X.; Yang, X. Q.; McBreen, J. *J. Electrochem. Soc.* **2000**, *147*, 2903.
- (4) Mansour, A. N.; McBreen, J.; Melendres, C. A. *J. Electrochem. Soc.* **1999**, *146*, 2799.
- (5) Mansour, A. N.; Croguennec, L.; Prado, G.; Delmas, C. *J. Synchrotron Rad.* **2001**, *8*, 866.
- (6) Mansour, A. N.; Yang, X. Q.; Sun, X.; McBreen, J.; Croguennec, L.; Delmas, C. *J. Electrochem. Soc.* **2000**, *147*, 2104.
- (7) Nakai, I.; Takahashi, K.; Shiraishi, Y.; Nakagome, T. *J. Phys. IV France* **1997**, *7 (C2)*, 1243.
- (8) Nakai, I.; Takahashi, K.; Shiraishi, Y.; Nakagome, T. J.; Izumi, F.; Ishii, Y.; Nishikawa, F.; Konishi, T. *J. Power Sources* **1997**, *68*, 536.
- (9) Nakai, I.; Nakagome, T. *J. Electrochem. Solid-State Lett.* **1998**, *1*, 259.
- (10) Nonaka, T.; Okuda, C.; Ukyo, Y.; Okamoto, T. *J. Synchrotron Rad.* **2001**, *8*, 869.
- (11) Montoro, L. A.; Abbate, M.; Rosolen, J. M. *J. Electrochem. Soc.* **2000**, *147*, 1651.
- (12) Montoro, L. A.; Abbate, M.; Rosolen, J. M. *Electrochem. Solid-State Lett.* **2000**, *3*, 410.
- (13) Uchimoto, Y.; Sawada, H.; Yao, T. *J. Power Sources* **2001**, *97/98*, 326.
- (14) Graetz, J.; Hightower, A.; Ahn, C. C.; Yazami, R.; Rez, P.; Fultz, B. *J. Phys. Chem. B* **2002**, *106*, 1286.
- (15) Yoon, W. S.; Kim, K. B.; Kim, M. G.; Lee, M. K.; Shin, H. J.; Lee, J. M.; Lee, J. S.; Yo, C. H. *J. Phys. Chem. B* **2002**, *106*, 2526.
- (16) Wolverton, C.; Zunger, A. *Phys. Rev. Lett.* **1998**, *81*, 606.
- (17) Aydinol, M. K.; Kohan, A. F.; Ceder, G.; Cho, K.; Joannopoulos, J. *J. Phys. Rev. B* **1997**, *56*, 1354.
- (18) Ceder, G.; Aydinol, M. K.; Kohan, A. F. *Comput. Mater. Sci.* **1997**, *8*, 161.
- (19) Van der Ven, A.; Aydinol, M. K.; Ceder, G.; Kresse, G.; Hafner, J. *J. Phys. Rev. B* **1998**, *58*, 2975.
- (20) Ronci, F.; Scrosati, B.; Rossi Albertini, V.; Perfetti, P. *J. Phys. Chem. B* **2001**, *105*, 754.
- (21) Egerton, R. F. *Electron Energy Loss Spectrometry in the Electron Microscope*; Plenum: New York, 1986.
- (22) Vvedensky, D. D.; Pendy, J. B. *Phys. Rev. Lett.* **1985**, *54*, 2725.
- (23) Rez, P.; Weng, X.; Ma, H. *Microsc. Microanal. Microstruct.* **1991**, *2*, 143.
- (24) Kurata, H.; Lefevre, E.; Coliex, C.; Brydson, R. *Phys. Rev. B* **1993**, *47*, 13763.
- (25) Stolojan, V.; Walsh, C. A.; Yuan, J.; Brown, L. M. *Inst. Phys. Conf. Ser.* **1999**, *161*, 235.
- (26) Pearson, D. H.; Fultz, B.; Ahn, C. C. *Appl. Phys. Lett.* **1988**, *53*, 1405.
- (27) Pearson, D. H.; Ahn, C. C.; Fultz, B. *Phys. Rev. B* **1992**, *47*, 8471.
- (28) Leapman, R. D.; Grunes, L. A.; Fejes, P. L. *Phys. Rev. B* **1981**, *26*, 614.
- (29) Sparrow, T. G.; Williams, B. G.; Rao, C. N. R.; Thomas, J. M. *Chem. Phys. Lett.* **1984**, *108*, 547.
- (30) Kuiper, P.; Kruizinga, G.; Ghijsen, J.; Sawatzky, G. A. *Phys. Rev. Lett.* **1989**, *62*, 221.
- (31) Pedio, M.; Fuggle, J. C.; Somers, J.; Umbach, E.; Haase, J.; Linder, Th.; Hofer, U.; Grioni, M.; de Groot, F. M. F.; Hillert, B.; Becker, L.; Robinson, A. *Phys. Rev. B* **1989**, *40*, 7924.
- (32) de Groot, F. M. F.; Grioni, M.; Fuggle, J. C.; Ghijsen, J.; Sawatzky, G. A.; Petersen, H. *Phys. Rev. B* **1989**, *40*, 5715.